

## An approximate solution for a pseudocapacitor

Venkat R. Subramanian<sup>a</sup>, Sheba Devan<sup>b</sup>, Ralph E. White<sup>b,\*</sup>

<sup>a</sup> Department of Chemical Engineering, Tennessee Tech University, 307 Prescott Hall, Cookeville, TN 38505, USA

<sup>b</sup> Department of Chemical Engineering, Center for Electrochemical Engineering, Swearingen Engineering Center, University of South Carolina, Columbia, SC 29208, USA

Received 16 February 2004; accepted 5 March 2004

Available online 10 June 2004

### Abstract

Transient analytical solutions are presented for the overpotential and the voltage for a porous electrode that includes both double-layer charging and a faradaic reaction. In addition, a simplified dynamic model is developed for the same process based on a second order, three-parameter polynomial approximate model. The effects of the parameters such as dimensionless exchange current density, conductivity ratio and applied current density on the voltage and overpotential distribution are presented. Also, using the exact transient solution an expression for the dimensionless interfacial current density is derived and the effects of the parameters mentioned above are presented.

© 2004 Elsevier B.V. All rights reserved.

**Keywords:** Capacitors; Polynomial approximation; Analytical solution; Porous electrode; Transient

### 1. Introduction

Capacitors have received considerable attention recently because of their high power densities [1]. Originally, capacitors served mainly as backup power sources for memories, microcomputers and clocks. Later they were used as main power sources in applications that required short pulses of large current for several seconds duration. Currently, they are employed in hybrid configurations with batteries and fuel cells. Capacitors can be broadly classified [2] as electrochemical double-layer capacitors or pseudocapacitors (i.e., an electrochemical capacitor with a faradaic reaction).

The performance of a capacitor depends on many factors such as the material properties, cell design and operating conditions. To fabricate capacitors for a particular application, it is necessary to analyze the performance and optimize the system parameters. Mathematical modeling has proven to be very useful for this purpose [3]. Both circuit analog models and macroscopic models [2–5] have been used to predict the behavior of capacitors. Circuit analog models do not capture the physics. While macroscopic models capture the physics, they are often time consuming to solve. Hence simplified models without compromising accuracy are highly desirable. In this paper, an approximate model for a pseudocapacitor is presented.

A pseudocapacitor cell can consist of two porous electrodes with a separator between them as illustrated in Fig. 1. The system is filled with electrolyte throughout. In this paper, we present a model for a single porous electrode. The objectives of this work are three-fold: (1) Develop an analytical solution for the transient behavior of a porous electrode with both double-layer charging and a faradaic reaction with linear kinetics. (2) Develop a simplified dynamic model to replace the transient solution obtained in (1). (3) Study the effect of the various parameters such as the exchange current density, conductivity ratio and applied current density on the developed model. The interfacial current density distribution across the electrode is a measure of the active material utilization. Based on the interfacial current density distribution, the performance of the capacitors can be optimized. Here, an expression for the interfacial current density is derived using the transient analytical solution. Using this expression the interfacial current distribution is determined as a function of the system parameters.

### 2. Model description

The following assumptions are made: (1) Porous electrode theory in one dimension is applicable. [6]. (2) No concentration gradients exist inside the electrode. (3) Both double-layer charging and a linear faradaic reaction occur. (4) The material and kinetic properties ( $a$ ,  $\sigma$ ,  $\kappa$ ,  $\alpha_a$ ,  $\alpha_c$

\* Corresponding author. Tel.: +1-803-777-3270; fax: +1-803-777-9597.  
E-mail address: [white@enr.sc.edu](mailto:white@enr.sc.edu) (R.E. White).

**Nomenclature**

$a$	specific interfacial area ( $\text{cm}^{-1}$ )
$a(\tau)$	time-dependent parameter of the simplified dynamic model (see Eq. (25))
$b(\tau)$	time-dependent parameter of the dynamic model (see Eq. (20))
$c(\tau)$	time-dependent parameter of the dynamic model (see Eq. (21))
$C_{dl}$	double-layer capacitance ( $\text{F}/\text{cm}^2$ )
$F$	Faraday's constant, 96487 C/eq.
$i_0$	exchange current density ( $\text{A}/\text{cm}^2$ )
$i_1$	matrix phase current density ( $\text{A}/\text{cm}^2$ )
$i_2$	solution phase current density ( $\text{A}/\text{cm}^2$ )
$I$	total cell current density ( $\text{A}/\text{cm}^2$ )
$j_n$	interfacial current density ( $\text{A}/\text{cm}^2$ )
$j_n^*$	dimensionless interfacial current density (see Eq. (43))
$j_{n,f}$	faradaic interfacial current density ( $\text{A}/\text{cm}^2$ )
$L$	thickness of the porous electrode (cm)
$n$	number of electrons transferred in the reaction
$R$	universal gas constant, 8.313 J/mol K
$t$	time (s)
$T$	temperature (K)
$V^*$	dimensionless voltage drop across the porous electrode
$x$	distance (cm)
$X$	dimensionless distance, $x/L$

**Greek symbols**

$\alpha_a, \alpha_c$	anodic and cathodic transfer coefficients respectively ( $\alpha_a + \alpha_c = n$ )
$\beta$	ratio of the solution phase and matrix phase conductivities, $\kappa/\sigma$
$\delta$	dimensionless current density, $I(FL/\kappa RT)$
$\eta$	overpotential ( $\phi_1 - \phi_2$ ) (V)
$\eta^*$	dimensionless overpotential, $\eta F/RT$
$\eta_{avg}^*$	average dimensionless overpotential (see Eq. (24))
$\kappa$	solution phase conductivity (S/cm)
$\nu^2$	dimensionless exchange current density $[ai_0(\alpha_a + \alpha_c)FL^2/RT](1/\sigma + 1/\kappa)$
$\sigma$	matrix phase conductivity (S/cm)
$\tau$	dimensionless time $t/(aC_{dl}(1/\kappa + 1/\sigma)L^2)$
$\phi_1$	solid phase potential (V)
$\phi_2$	solution phase potential (V)
$\phi_1^*$	dimensionless solid phase potential, $\phi_1 F/RT$

and  $i_0$ ) are assumed to be constants. (5) The double-layer capacitance ( $C_{dl}$ ) is taken to be a constant. (6) The open circuit potential is set equal to zero. With no concentration gradients, the matrix phase current density,  $i_1$  and solution phase current density,  $i_2$  are given by Ohm's law [6]:

$$i_1 = -\sigma \frac{\partial \phi_1}{\partial x} \quad (1)$$

$$i_2 = -\kappa \frac{\partial \phi_2}{\partial x} \quad (2)$$

where  $\sigma$  and  $\kappa$  are the matrix phase and solution phase conductivities, respectively. The total current density  $I$  is the sum of the matrix and solution phase current densities:

$$i_1 + i_2 = I \quad (3)$$

where  $I$  is the applied current density under galvanostatic conditions (note that  $I$  is defined to be positive when leaving the current collector at  $x = L$ , see Fig. 1). The current transferred from the matrix phase to the solution phase is expressed in terms of the interfacial current density,  $j_n$  [6]:

$$-\frac{\partial i_1}{\partial x} = \frac{\partial i_2}{\partial x} = aj_n \quad (4)$$

where  $a$  is the surface area per unit volume of the porous electrode. The interfacial current density ( $j_n$ ) is the sum of the double-layer charging current density and the faradaic current density:

$$j_n = C_{dl} \frac{\partial(\phi_1 - \phi_2)}{\partial t} + j_{n,f} \quad (5)$$

where  $C_{dl}$  is the double-layer capacitance and the faradaic current density ( $j_{n,f}$ ) is given by the linear kinetic expression:

$$j_{n,f} = \frac{i_0 F(\alpha_a + \alpha_c)}{RT} (\phi_1 - \phi_2) \quad (6)$$

where  $\alpha_a + \alpha_c = n$  [6] and the open circuit potential has been set equal to zero. Substituting Eq. (6) in Eq. (5) yields

$$j_n = C_{dl} \frac{\partial(\phi_1 - \phi_2)}{\partial t} + \frac{i_0(\alpha_a + \alpha_c)F}{RT} (\phi_1 - \phi_2) \quad (7)$$

Let the overpotential be given by  $\eta = \phi_1 - \phi_2$ . The initial and boundary conditions for the overpotential are given by [5]:

$$\phi_1 = 0 \quad \text{and} \quad \phi_2 = 0 \Rightarrow \eta = 0 \quad \text{at} \quad t = 0 \quad \text{for} \quad 0 \leq x \leq L \quad (8)$$

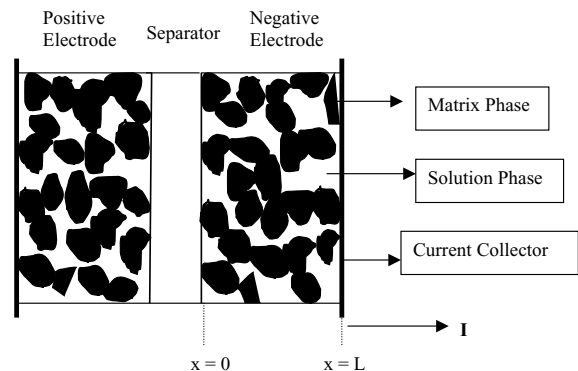


Fig. 1. Schematic of an electrochemical capacitor.

$$i_1 = 0 \quad \text{and} \quad i_2 = I \Rightarrow \frac{\partial \eta}{\partial x} = \frac{I}{\kappa} \quad \text{at } x = 0 \quad \text{for } t > 0 \quad (9)$$

$$i_1 = I \quad \text{and} \quad i_2 = 0 \Rightarrow \frac{\partial \eta}{\partial x} = -\frac{I}{\sigma} \quad \text{at } x = L \quad \text{and} \quad \text{for } t > 0 \quad (10)$$

Eqs. (1), (2), (4) and (7) can be used to determine the following equation for the overpotential in dimensionless form:

$$\frac{\partial \eta^*}{\partial \tau} = \frac{\partial^2 \eta^*}{\partial X^2} - v^2 \eta^* \quad (11)$$

where  $v^2$  (dimensionless exchange current density) [6] is

$$v^2 = \frac{ai_0(\alpha_a + \alpha_c)FL^2}{RT} \left( \frac{1}{\sigma} + \frac{1}{\kappa} \right) \quad (12)$$

and

$$X = \frac{x}{L}, \quad \tau = \frac{t}{aC_{dl}(1/\kappa + 1/\sigma)L^2}, \quad \eta^* = \frac{\eta F}{RT} \quad (13)$$

The corresponding dimensionless initial and boundary conditions are

$$\eta^* = 0 \quad \text{at } \tau = 0 \quad \text{and} \quad \text{for } 0 \leq X \leq 1 \quad (14)$$

$$\frac{\partial \eta^*}{\partial X} = \delta \quad \text{at } X = 0 \quad \text{and} \quad \text{for } \tau > 0 \quad (15)$$

$$\frac{\partial \eta^*}{\partial X} = -\delta\beta \quad \text{at } X = 1 \quad \text{and} \quad \text{for } \tau > 0 \quad (16)$$

where  $\beta$  is the ratio of the solution phase to matrix phase conductivity ( $\beta = \kappa/\sigma$ ) and  $\delta$  is the dimensionless current density:

$$\delta = I \left( \frac{FL}{\kappa RT} \right) \quad (17)$$

### 2.1. Exact transient solution

An exact transient solution for this model can be derived using the separation of variables method [7] and is given by

$$\eta^* = \frac{\delta(1 + \beta) e^{-v^2 \tau}}{v^2} - \frac{\delta[\cosh(v[1 - X]) + \beta \cosh(vX)]}{v \sinh(v)} + 2\delta \sum_{n=1}^{\infty} A_n \cos(n\pi X) e^{-(n^2 \pi^2 + v^2) \tau} \quad (18)$$

where  $A_n = (\beta \cos(n\pi) + 1)/(v^2 + n^2 \pi^2)$

The number of terms required for convergence of this series can be significant and depends strongly on the dimensionless current density  $\delta$ .

### 2.2. Simplified dynamic model

An approximate solution for the same model (Eq. (11) subject to Eqs. (14)–(16) can be found by assuming that the dimensionless overpotential is a polynomial in  $X$  [8]:

$$\eta^*(X, \tau) = a(\tau) + b(\tau)X + c(\tau)X^2 \quad (19)$$

where  $a(\tau)$ ,  $b(\tau)$  and  $c(\tau)$  may be functions of the dimensionless time. Two of these time-dependent parameters ( $b(\tau)$  and  $c(\tau)$ ) can be determined using the boundary conditions. By applying Eq. (19) to the boundary condition at  $X = 0$  we get

$$b(\tau) = \delta \quad (20)$$

Similarly,  $c(\tau)$  can be obtained by using the boundary condition at  $X = 1$  as follows:

$$c(\tau) = -\frac{1}{2}\delta(1 + \beta) \quad (21)$$

An average  $\eta^*$  can be determined by using Eq. (19):

$$\eta_{\text{avg}}^* = \int_0^1 \eta^* dX = a(\tau) + \frac{b(\tau)}{2} + \frac{c(\tau)}{3} \quad (22)$$

Eq. (11) together with Eqs. (19) and (21) can be used to derive an equation for the time dependence of the dimensionless average overpotential,  $\eta_{\text{avg}}^*$ . First, use Eqs. (19) and (21) to obtain an expression for the second derivative of  $\eta^*$  with respect to  $X$ . Next, put this expression into Eq. (11) and integrate both sides of the resulting equation with respect to  $X$  from  $X = 0$  to 1. The result is

$$\frac{d\eta_{\text{avg}}^*}{d\tau} = -\delta(1 + \beta) - v^2 \eta_{\text{avg}}^* \quad (23)$$

Eq. (23) can be solved by using the initial condition  $\eta^* = 0$  at  $\tau = 0$  for all  $X$  to obtain

$$\eta_{\text{avg}}^* = e^{-v^2 \tau} \frac{\delta(1 + \beta)}{v^2} - \frac{\delta(1 + \beta)}{v^2} \quad (24)$$

Next, the time-dependent parameter  $a(\tau)$  can be determined by substituting Eqs. (20), (21) and (24) into Eq. (22). The result is

$$a(\tau) = e^{-v^2 \tau} \frac{\delta(1 + \beta)}{v^2} - \frac{\delta(1 + \beta)}{v^2} + \frac{\delta\beta}{6} - \frac{\delta}{3} \quad (25)$$

The dimensionless overpotential based on the polynomial approximation (simplified dynamic model) is obtained by substituting  $a(\tau)$ ,  $b(\tau)$  and  $c(\tau)$  into Eq. (19). The result is

$$\eta^* = -\frac{\delta}{3} + \frac{\delta\beta}{6} + e^{-v^2 \tau} \frac{\delta(1 + \beta)}{v^2} - \frac{\delta(1 + \beta)}{v^2} + \delta X - \frac{\delta(1 + \beta)}{2} X^2 \quad (26)$$

Comparing Eq. (18) to Eq. (27) shows that the simplified dynamic model does not contain an infinite series and is, consequently, much simpler. Note that the simplified dynamic model involves all the physical and kinetic parameters of the model.

### 2.3. Potential drop across the electrode

Combining Eqs. (1), (4) and (7) gives the equation for solid phase potential as

$$\sigma \frac{\partial^2 \phi_1}{\partial x^2} = aC_{dl} \frac{\partial \eta}{\partial t} + \frac{ai_0(\alpha_a + \alpha_c)F}{RT} \eta \quad (27)$$

Substitution of the dimensionless variables as defined in Eq. (13) into Eq. (27) and letting

$$\phi_1^* = \frac{\phi_1 F}{RT} \quad (28)$$

yields an equation for the dimensionless solid phase potential

$$\frac{\partial^2 \phi_1^*}{\partial X^2} = \frac{\beta}{1 + \beta} \left[ \frac{\partial \eta^*}{\partial \tau} + \nu^2 \eta^* \right] \quad (29)$$

Using Eq. (11), Eq. (29) can be rewritten as

$$\frac{\partial^2 \phi_1^*}{\partial X^2} = \frac{\beta}{1 + \beta} \frac{\partial^2 \eta^*}{\partial X^2} \quad (30)$$

The boundary conditions for  $\phi_1^*$  and  $\eta^*$  in Eq. (30) are

$$\frac{\partial \phi_1^*}{\partial X} = 0 \quad \text{and} \quad \frac{\partial \eta^*}{\partial X} = \delta \quad \text{at} \quad X = 0 \quad (31)$$

$$\frac{\partial \phi_1^*}{\partial X} = -\delta\beta \quad \text{and} \quad \frac{\partial \eta^*}{\partial X} = -\delta\beta \quad \text{at} \quad X = 1 \quad (32)$$

Eq. (30) can be integrated once with respect to  $X$  to yield

$$\frac{\partial \phi_1^*}{\partial X} = \frac{\beta}{1 + \beta} \frac{\partial \eta^*}{\partial X} + C \quad (33)$$

where  $C$  is an integration constant that can be determined using one of the boundary conditions (Eq. (31) or (32)):

$$C = -\frac{\delta\beta}{1 + \beta} \quad (34)$$

Integrating Eq. (34) between the limits  $X = 0$  to  $1$  gives the change in the dimensionless solid phase potential across the electrode

$$\phi_1^*|_{X=1} - \phi_1^*|_{X=0} = \frac{\beta}{1 + \beta} (\eta^*|_{X=1} - \eta^*|_{X=0}) - \frac{\delta\beta}{1 + \beta} \quad (35)$$

The potential drop across the porous electrode can be defined as

$$V^* = (\phi_1^*|_{X=1} - \phi_2^*|_{X=0}) \quad (36)$$

or

$$V^* = (\phi_1^*|_{X=1} - \phi_1^*|_{X=0}) + \eta^*|_{X=0} \quad (37)$$

By substituting Eq. (35) into Eq. (37), we get the dimensionless voltage drop across the electrode as

$$V^* = \left[ \frac{\eta^*|_{X=0} + \beta\eta^*|_{X=1} - \delta\beta}{1 + \beta} \right] \quad (38)$$

This dimensionless voltage across the porous electrode ( $V^*$ ) from  $X = 1$  to  $X = 0$  can be determined by using the exact

transient solution (Eq. (18)) as

$$V^* = \frac{\delta(1 + \beta) e^{-\nu^2 \tau}}{\nu^2} - \frac{\delta\beta}{1 + \beta} - \frac{\delta [(1 + \beta^2) \cosh(\nu) + 2\beta]}{\nu \sinh(\nu)(1 + \beta)} + 2\delta \sum_{n=1}^{\infty} B_n e^{-(n^2 \pi^2 + \nu^2) \tau} \quad (39)$$

where

$$B_n = \frac{(\beta \cos(n\pi) + 1)^2}{\nu^2 + n^2 \pi^2}$$

The dimensionless voltage drop across the porous electrode from  $X = 1$  to  $X = 0$  as determined by using the simplified dynamic model (Eq. (27)) consists of only two terms:

$$V^* = \frac{\delta(1 + \beta)[e^{-\nu^2 \tau} - 1]}{\nu^2} - \frac{\delta(1 + \beta)}{3} \quad (40)$$

### 2.4. Interfacial current density

Substituting for  $i_1$  in Eq. (4), from Eq. (1) gives the interfacial current density as

$$j_n = \frac{1}{a\sigma} \frac{\partial^2 \phi_1}{\partial x^2} \quad (41)$$

Introducing the dimensionless variable  $\phi_1^*$  (Eq. (28) and X Eq. (13)) into Eq. (41) gives the dimensionless interfacial current density ( $j_n^*$ ).  $j_n^*$  can be written in terms of the dimensionless overpotential using Eq. (30):

$$j_n^* = \frac{1}{\beta + 1} \frac{\partial^2 \eta^*}{\partial X^2} \quad (42)$$

Evaluating the second derivative of the dimensionless overpotential with respect to the distance from Eq. (18) gives the expression for  $j_n^*$  as

$$j_n^* = -2\delta \sum_{n=1}^{\infty} \frac{\beta \cos(n\pi) + 1}{(\nu^2 + n^2 \pi^2)(\beta + 1)} n^2 \pi^2 \cos(n\pi X) e^{-(n^2 \pi^2 + \nu^2) \tau} - \frac{\delta \nu [\cosh(\nu[1 - X]) + \beta \cosh(\nu X)]}{(\beta + 1) \sinh(\nu)} \quad (43)$$

## 3. Results and discussion

From the equations presented above, it is clear that both overpotential and voltage drop across the porous electrode are functions of the dimensionless current density  $\delta$ , dimensionless exchange current density  $\nu^2$  and the ratio of conductivities  $\beta$ . The distribution of the overpotential across the porous electrode obtained from the transient solution is compared to the solution obtained using the simplified dynamic model in Fig. 2 for the parameter values  $\delta = -1$ ,  $\nu^2 = \beta = 1$ . This figure also shows the overpotential distribution at different dimensionless times. The change in

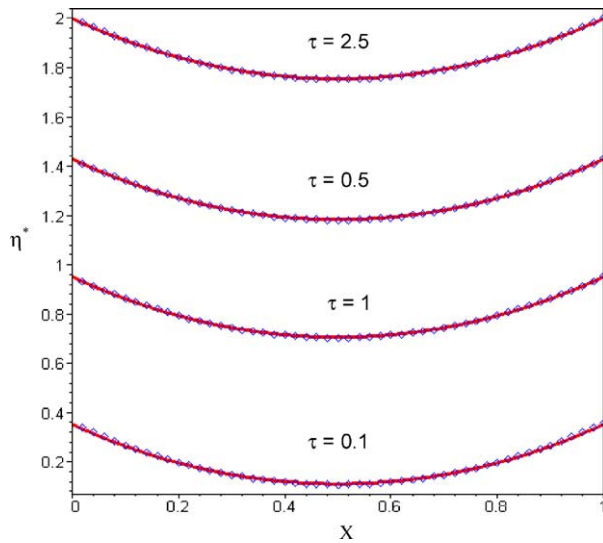


Fig. 2. Distribution of over potential across the porous electrode ( $v^2 = \beta = 1, \delta = -1$ ). The exact solution (continuous line) and the simplified dynamic model solution (symbols) agree well.

voltage drop across the porous electrode with time is plotted using both the exact solution and the simplified dynamic solution in Fig. 3. The voltage increases linearly at short times and levels off. The voltage profiles are similar to the transient potential response of insertion electrodes with linear kinetics and double-layer charging as shown by Ong and Newman (Fig. 5 of ref. [5]).

It is worth noting that Eq. (18) can be simplified as Eq. (44), when the pseudocapacitor involves only

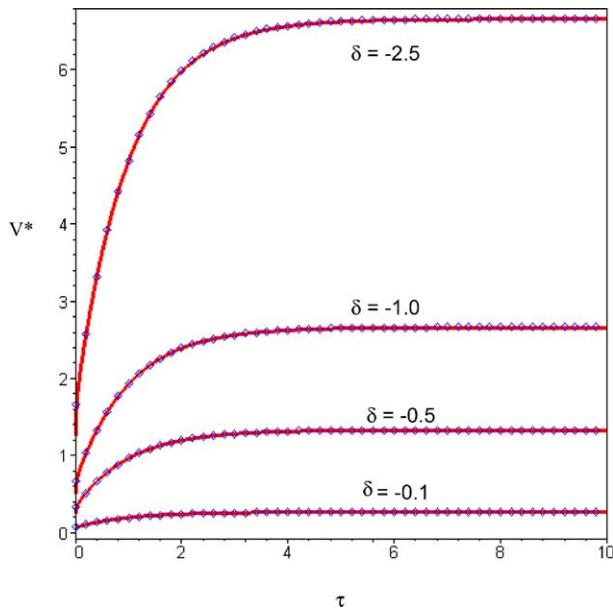


Fig. 3. Change in voltage across the porous electrode with dimensionless time ( $v^2 = \beta = 1$ ). The exact solution (continuous line) and the simplified dynamic model solution (symbols) agree well.

double-layer charging (i.e.,  $v^2 \rightarrow 0$ ):

$$\eta^* = -\delta(1 + \beta)\tau - \frac{\delta}{6}(3X^2 - 6X + 2) - \frac{\delta\beta}{6}(3X^2 - 1) + 2\delta \sum_{n=1}^{\infty} \frac{\cos(n\pi X)(\beta \cos(n\pi) + 1) e^{-n^2\pi^2\tau}}{n^2\pi^2} \quad (44)$$

It can be shown that Eq. (44) is equivalent to Eq. (16) given by Srinivasan and Weidner [2] provided the boundary conditions and the dimensionless variables given here are redefined according to those given in ref. [2]. Similarly when  $v^2 \rightarrow 0$ , Eq. (39) reduces to the voltage expression given in Eq. (45):

$$V^* = -\delta\tau(\beta + 1) - \frac{\delta}{3}(\beta + 1) + \sum_{n=1}^{\infty} \frac{2\delta(\beta \cos(n\pi) + 1)^2}{n^2\pi^2(\beta + 1)} e^{-n^2\pi^2\tau} \quad (45)$$

Eq. (45) is equivalent to Eq. (15) of ref. [2] when the initial voltage on discharge is assumed to be equal to zero. Hence the transient model developed for the pseudocapacitor reduces to that of the double-layer capacitor when the kinetics of the faradaic reaction is negligible ( $v^2 \rightarrow 0$ ). The voltage profiles for a pseudocapacitor are compared to that of a double-layer capacitor for different values of the discharge current density in Fig. 4. Newman pointed out that for large values of the dimensionless exchange current density ( $v^2$ ) and the dimensionless applied current density ( $\delta$ ), the ohmic effects dominate and the reaction distribution is non-uniform

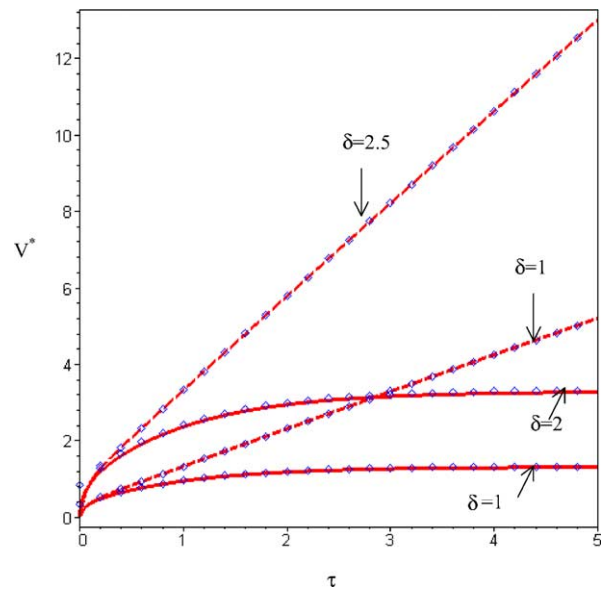


Fig. 4. The effect of dimensionless exchange current ( $v^2$ ) density on the voltage profile across the porous electrode for  $\beta = 0$ . The dimensionless applied current density ( $\delta$ ) are as indicated in the figure. Dotted lines are the voltage profile for  $v^2 = 0.01$  simulated using the exact solution. Solid lines are the voltage profile for  $v^2 = 1$  simulated using the exact solution. The exact solution (line) and the simplified dynamic model solution (symbols) agree well.

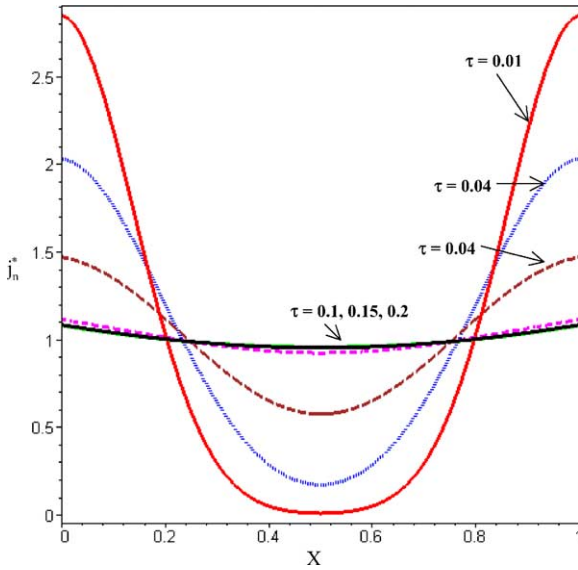


Fig. 5. Distribution of dimensionless interfacial current density ( $j_n^*$ ) for  $v^2 = \beta = 1$ ,  $\delta = -1$  and at different dimensionless times.  $j_n^*$  (Eq. (43)) is derived using the exact solution for the overpotential.

[6]. The dimensionless interfacial current ( $j_n^*$ ) distribution for  $v^2 = 1$  is illustrated in Fig. 5 at different  $\tau$ . The distribution of  $j_n^*$  reaches a steady state when  $\tau > 0.15$ . Compared to the steady state  $j_n^*$  distribution for  $v^2 = 0.01$  (small value of the dimensionless exchange current density) as shown in Fig. 6, it is clear that the steady state reaction distribution is non-uniform for  $v^2 = 1$ . The steady state distribution of  $j_n^*$  for  $v^2 = 0.01$  (Fig. 6) is more uniform and corresponds to reaction distribution of the double-layer capacitors [2]. The effect of  $\delta$  on the reaction distribution is given in Fig. 7. For

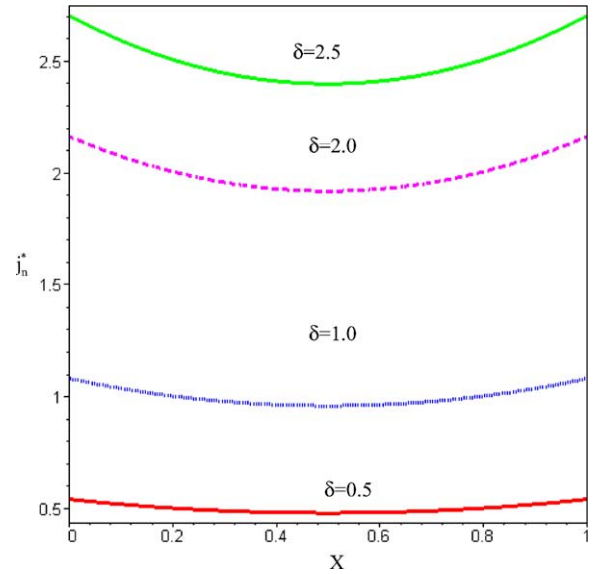


Fig. 7. The effect of dimensionless applied current density on the distribution of dimensionless interfacial current density ( $j_n^*$ ) for  $v^2 = \beta = 1$ ,  $\delta = -1$ .  $j_n^*$  (Eq. (43)) is derived using the exact solution for the overpotential.

higher values of the discharge current density the reaction distribution becomes non-uniform. The effect of the conductivity ratio ( $\beta$ ) on the reaction current density is to shift the reaction from one face to another [6]. This is evident from the plot of the reaction distribution for low value of  $\beta$  as given in Fig. 8. For  $\beta = 0$ , solid phase conductivity is higher than the solution phase conductivity, the reaction rate is higher at the solution/porous electrode interface. The reaction distribution for  $\beta = 10$ , where the solution phase conductivity is higher than the solid phase conductivity the profiles are

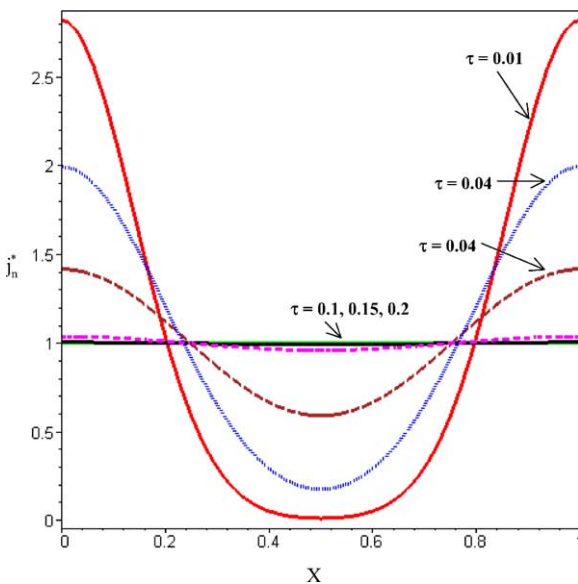


Fig. 6. Distribution of dimensionless interfacial current density ( $j_n^*$ ) for  $v^2 = 0.01$ ,  $\beta = 1$ ,  $\delta = -1$  and at different dimensionless times.  $j_n^*$  (Eq. (43)) is derived using the exact solution for the overpotential.

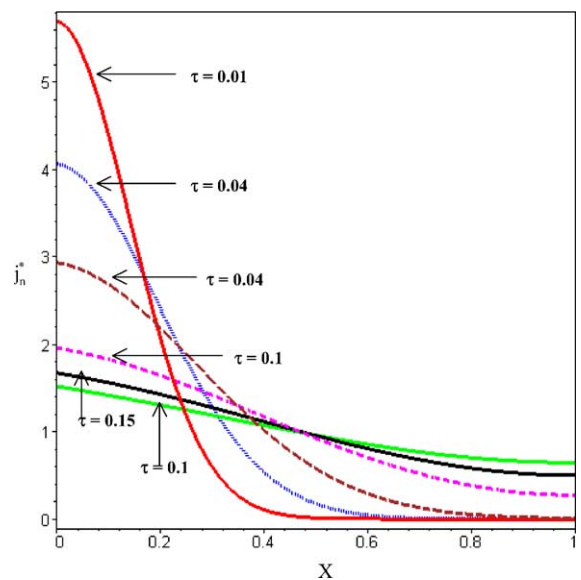


Fig. 8. Distribution of dimensionless interfacial current density ( $j_n^*$ ) for  $v^2 = 1$ ,  $\beta = 0$ ,  $\delta = -1$  and at different dimensionless times.  $j_n^*$  (Eq. (43)) is derived using the exact solution for the overpotential.

a mirror image of the plots for  $\beta = 0$ . Hence the reaction rate is higher at the porous electrode/current collector interface.

#### 4. Conclusion

An analytical solution for a macroscopic model of a porous electrode with linear kinetics was compared to a simplified dynamic model. Comparing the results, it was shown that the simplified dynamic or approximate model agrees well with the exact transient model for the chosen parameters ( $\nu^2 = \beta = 1$ ). The model includes both double-layer charging and a faradaic process approximated by linear kinetics. The exact transient analytical solution for the overpotential was used to determine the dimensionless interfacial current density (Eq. (43)). The dimensionless interfacial current density distribution is analyzed as a function of the parameters ( $\nu^2$ ,  $\beta$  and  $\delta$ ). A rigorous error analysis based on the parameters  $\delta$ ,  $\beta$  and  $\nu$  could be done as in ref. [7]. This analysis would determine the range of the parameters for which Eq. (27) could be used safely. In

addition, polynomial approximations of higher order [8] could be used to increase the accuracy.

#### Acknowledgements

The authors are grateful for the financial support of the project by National Reconnaissance Organization (NRO) under contract # NRO 000-03-C-0122.

#### References

- [1] R. Kotz, M. Carlen, J. Electrochem. Soc. 45 (2000) 2483.
- [2] V. Srinivasan, J.W. Weidner, J. Electrochem. Soc. 146 (1999) 1650.
- [3] C. Lin, J.A. Ritter, B.N. Popov, R.E. White, J. Electrochem. Soc. 146 (1999) 3168.
- [4] D. Dunn, J. Newman, J. Electrochem. Soc. 147 (2000) 820.
- [5] I.J. Ong, J. Newman, J. Electrochem. Soc. 146 (1999) 4360.
- [6] J.S. Newman, Electrochemical Systems, 2nd ed., Prentice-Hall, Englewood Cliffs, NJ, 1991.
- [7] V.R. Subramanian, R.E. White, J. Power Sources 96 (2001) 385.
- [8] V.R. Subramanian, J.A. Ritter, R.E. White, J. Electrochem. Soc. 148 (2001) E444.